Available online at www.sciencedirect.com
ScienceDirect
Advances in Space Research 40 (2007) 1–10
ADVANCES IN SPACE RESEARCH (a COSPAR publication)
www.elsevier.com/locate/asr

On-orbit performance of Gravity Probe B drag-free translation control and orbit determination

J. Li *, W.J. Bencze, D.B. DeBra, G. Hanuschak, T. Holmes, G.M. Keiser, J. Mester, P. Shestople, H. Small

Gravity Probe B Program, W.W. Hansen Experimental Physics Lab, Stanford University, Stanford, CA 94305, USA

Received 2 November 2006; received in revised form 6 March 2007; accepted 6 March 2007

Abstract

The Gravity Probe B (GP-B) Relativity Mission is a fundamental physics experiment to test Einstein's theory of General Relativity based on observations of spinning gyroscopes onboard a satellite in a near-polar, near-circular orbit at an altitude of about 640 km around the Earth. The GP-B mission was designed to test two predictions of Einstein's theory, the geodetic effect and the frame-dragging effect, to an accuracy better than 5×10^{-4} arcsec/yr. Drag-free control technology is implemented in the GP-B translation control system to minimize support forces and support induced torques on the gyroscopes. A Global Positioning System (GPS) receiver onboard the GP-B satellite provides real-time position, velocity and timing data. The GP-B orbit is determined on the ground based on the 3-axis GPS position data and verified independently with ground-based laser ranging measurements. This paper describes the design and implementation of the drag-free translation control and orbit determination system of the GP-B satellite. The on-orbit performance of the drag-free translation control system satisfies the requirements of the GP-B science experiment. The residual accelerations from the gyroscope control efforts are less than 4×10^{-11} m/s^2 (along the satellite roll axis) and less than 2×10^{-10} m/s^2 (transverse to the satellite roll axis) between 0.01 mHz and 10 mHz in inertial space. The non-gravitational acceleration along the satellite roll axis, including a nearly constant component (which is kept below 1×10^{-7} m/s^2) and a sinusoidal component (whose amplitude varies from about 5×10^{-7} m/s^2 to less than 1×10^{-8} m/s^2), causes the gyroscope spin axis to drift less than 9×10^{-5} arcsec/yr. The orbit determination system is found to provide overlapping orbit solution segments having RMS (root mean square) position and velocity errors of a few meters and a few mm/s, well within the RMS mission requirements of 25 m and 7.5 cm/s.

Keywords: Gravity Probe B (GP-B); General Relativity; Drag-free control; Orbit determination; SLR; On-orbit performance

1. Introduction

The Gravity Probe B (GP-B) Relativity Mission is a fundamental physics experiment to test two predictions of Einstein's theory of General Relativity based on observations of spinning gyroscopes onboard a satellite in a near-polar, near-circular orbit at an altitude of about 640 km around the Earth (Everitt, 1988; Everitt et al., 2001). In Newton's gravitational theory, the spin axes of the gyroscopes remain fixed in inertial space if there are no torques on the gyroscopes. However, for the GP-B orbit, it is predicted by General Relativity that the spin axes of the gyroscopes drift by 6.6 arcsec/yr in the orbital plane due to the mass of the Earth and drift by 0.041 arcsec/yr perpendicular to the orbital plane due to the rotation of the Earth, as illustrated in Fig. 1. These are called the geodetic effect and the frame-dragging effect, respectively. The GP-B mission was designed to measure the two relativistic effects to an accuracy better than 5×10^{-4} arcsec/yr.

The GP-B satellite was successfully launched into orbit on April 20, 2004. The GP-B experiment consists of three phases: the initialization phase for 128 days, the science data collection phase for 353 days and the calibration phase for 46 days. The science data collection started from

* Corresponding author. Tel.: +1 650 725 6388; fax: +1 650 725 8312.
E-mail address: li@relgyro.stanford.edu (J. Li).

0273-1177/$30 © 2007 Published by Elsevier Ltd on behalf of COSPAR.
doi:10.1016/j.asr.2007.03.009

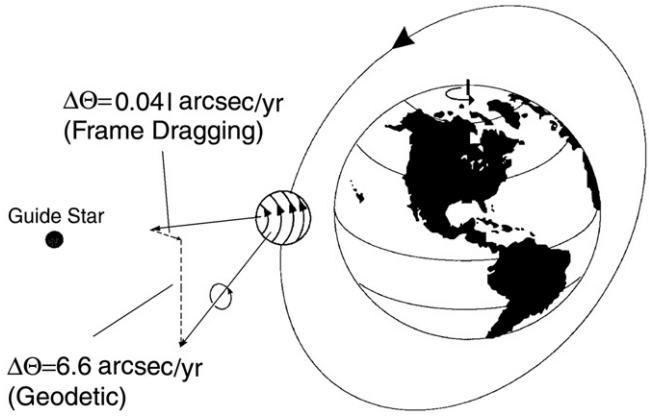

Fig. 1. The Gravity Probe B Relativity Mission.

August 28, 2004. The GP-B on-orbit experiment was completed on September 29, 2005 when the superfluid helium dewar was depleted.

The GP-B satellite rolls at a period of 77.5 s about an axis toward a guide star, IM Pegasi, which lies within 0.1 degree of the orbital plane during the GP-B experiment. A telescope tracks the guide star. The spin axes of the gyroscopes are initially aligned to within 20 arcsec of the guide star. The long term drift in the spin axis orientation of the gyroscopes is measured relative to the guide star. In the science data collection phase, the translation control system employs the drag-free control technology, which minimizes the support forces and support induced torques on the gyroscopes. A Global Positioning System (GPS) receiver onboard the GP-B satellite provides real-time position, velocity and timing data. The GP-B orbit is determined on the ground based on the 3-axis GPS position data and verified independently with ground-based laser ranging measurements provided by the International Laser Ranging Service (Pearlman et al., 2002).

This paper is organized as follows: first, the drag-free control is introduced and the translation control system is described. Second, the orbit determination system is presented and the force modeling is discussed. Third, the flight data are shown to demonstrate the on-orbit performance. Finally, conclusions are provided.

2. Drag-free translation control

DeBra (2003) discussed the drag-free control technology for fundamental physics experiments in space. A drag-free control system comprises a proof mass free floating in the satellite, a sensor to measure any displacements between the proof mass and the satellite, a number of low-level (ideally proportional) thrusters as actuators, and the associated electronics and software (drag-free control algorithms). The shielded proof mass within the satellite follows a purely gravitational orbit. The satellite is controlled to follow the proof mass by the thrusters, which produce a force equal and opposite to the disturbances to the satellite, i.e., air drag, radiation pressure, micrometeorite impacts, etc. Therefore, the drag-free control provides a dynamically quiet platform for high-precision experiments. The principle of the drag-free satellite was conceived by Pugh (1959) and further developed by Lange (1964). The first drag-free satellite was the Triad, one of the TRANSIT navigation satellites of the Navy Navigation Satellite System. The Triad was developed by Applied Physics Lab of John Hopkins University and Guidance and Control Lab of Stanford University (1974). It was demonstrated that the residual acceleration of the Triad satellite was 5×10^{-11} m/s^2 in the flight in 1972.

The GP-B experiment was designed to reduce the Newtonian drift of the gyroscope below 5×10^{-4} arcsec/yr. To achieve this goal, drag-free control is necessary to minimize the gyroscope support induced torques. The uncompensated forces are mostly constant or at orbital or twice orbital frequency in the axes of the satellite body-fixed frame. Along the direction of the gyroscope spin axis these are averaged at the spin frequency and contribute relatively little to the gyroscope drift error budget. The amplitude of the disturbance forces falls off significantly with frequency. Thus the satellite was designed to roll about the line of sight to the guide star in order to spectrally shift the science data (which is in inertial space) with respect to these disturbances. As a result, the disturbances transverse to the gyroscope spin axis are now averaged at the roll frequency and the modest amount of disturbance at the roll frequency is acceptably low. The gyroscope spin axis is within 30 arcsec of the satellite roll axis during the GP-B flight. As long as the residual accelerations of the GP-B satellite are less than 2×10^{-6} m/s^2 along the satellite roll axis and less than 4×10^{-10} m/s^2 transverse to the satellite roll axis in inertial space, the Newtonian drift of the gyroscope is less than 5×10^{-4} arcsec/yr.

There are 4 gyroscopes onboard the GP-B satellite. Any one of them can be used as the proof mass for the drag-free control system. The mass center of the GP-B satellite is approximately 23 cm away from the location of the first gyroscope. Each subsequent gyroscope is 8.8 cm further from the satellite mass center along the satellite roll axis. The acceleration due to the gradient of the Earth's gravitational field is on the order of 4×10^{-7} m/s^2 on the first gyroscope and increases linearly with the distance between the satellite mass center and the other gyroscopes. Drag-free control in effect moves the point of free fall from the satellite mass center to the location of the gyroscope used as the proof mass. This reduces the gravity gradient acceleration on the other gyroscopes as well.

Fig. 2 shows a photograph of the GP-B gyroscope and housing. The diameter of the gyroscope is 38 mm and the gap between the gyroscope and the housing is 32 μm. The position of the gyroscope with respect to the housing is measured in three axes with a capacitance bridge to a noise floor of 1.5 nm/$\sqrt{\text{Hz}}$ and quantized at the level of 1 nm. The Gyroscope Suspension System (GSS) keeps the gyroscope at the center of the housing by servo-controlled electrostatic

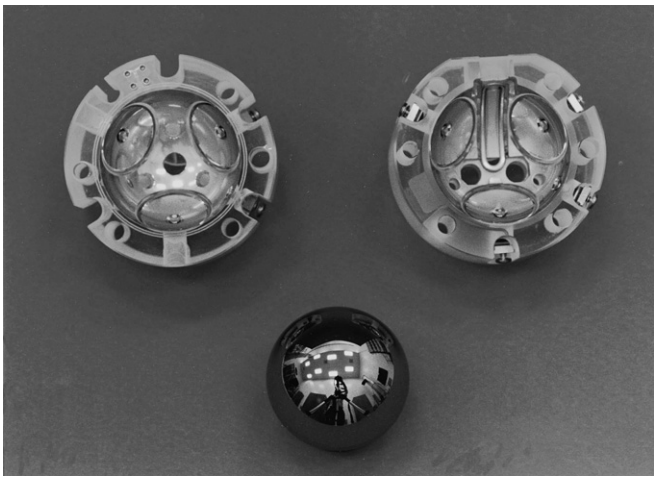

Fig. 2. GP-B gyroscope and housing.

forces applied to a set of 6 electrodes. The drag-free control is implemented with 16 proportional cold gas thrusters, which use the exhaust gas boil-off from the superfluid helium dewar of the GP-B satellite as the propellant. The maximum thrust of the thrusters is 10 mN. A typical operating point is 8.5 mN for a mass flow of 6 mg/s, representing a specific impulse of 130 s. The thrust noise is measured to be 25 $\mu N/\sqrt{Hz}$. The bias variation of the thrusters is less than 0.2 mN and the scale factor variation is less than 6%.

The drag-free control can be implemented in two modes: the free floating mode and the accelerometer mode. In the free floating mode, active gyroscope suspension control is disabled, the gyroscope position with respect to the housing is fed back to the translation control system, and the drag-free control minimizes the relative position between the gyroscope and the satellite. In the accelerometer mode, the gyroscope suspension control is enabled, the gyroscope suspension control effort is fed back to the translation control system, and the drag-free control minimizes the gyroscope suspension control effort. Fig. 3 shows the diagram of the drag-free translation control system in the free floating mode (Fig. 3a) and the accelerometer mode (Fig. 3b), respectively.

In the free floating mode, the suspension forces and the related torques on the gyroscope used as the proof mass are minimal, which is of great value for the GP-B experiment. However, implementing drag-free control in the accelerometer mode has several engineering advantages: first, the spinning gyroscope is always actively centered by the GSS, and thus is at minimal risk of contacting the housing wall. Second, the bias of the residual acceleration can be compensated. Finally, the larger torques due to the active suspension are well within the requirements, and the three gyroscopes other than the one used as the proof mass need to be suspended against the gravity gradient in any case in the free floating mode. Considering the above factors, the GP-B drag-free translation control system was implemented in the accelerometer mode when the science data were collected.

A more detailed description of the GP-B drag-free translation control system was given by Bencze et al. (2006).

3. Orbit determination

Accurate orbit data for the GP-B satellite are required not only for mission operations but also for the science data processing. The RMS (root mean square) position and velocity errors should be less than 25 m and 7.5 cm/s, respectively, for an accurate calibration of the GP-B science measurements and a comparison of the measured relativistic drift rates of the spin axes of the gyroscopes with the predicted drift rates.

The GPS equipment onboard the GP-B satellite is divided into two fully redundant sets. Each set comprises a receiver and 4 antennas, manufactured by Trimble Navigation Limited (http://www.trimble.com) and modified for space use by Stanford University and Lockheed Martin Company. Each receiver has 6 channels for the L1 signal, from which real-time position, velocity and timing data are calculated onboard the GP-B satellite and sent to the ground via telemetry. The combined field-of-view of the set of 4 antennas covers the entire sky so that the GPS receiver is able to track the GPS satellites continuously while the GP-B satellite rolls. Shestople et al. (2004) discussed the hardware and software of the GPS receiver onboard the GP-B satellite and showed the on-orbit performance in the initialization phase of the GP-B experiment.

The GP-B orbit is determined on the ground, using the 3-axis GPS position data at 10-second intervals in the commercial software package MicroCosm developed by Van Martin Systems, Inc. (http://www.vmsi-microcosm.com). The position data were divided into 18-hour spans which are centered on 06:00 and 18:00 hours each day, so there are 6-hour overlaps at the ends of each span. GP-B ephemeris segments are generated from each data span using independent batch fits to the 6 state variables of position and velocity and five additional coefficients used for axial force modeling. The 6-hour overlaps at the start and end of the data span allow for consistency comparisons and end-effect studies.

The force modeling includes a 50×50 GGM02C geopotential model (Tapley et al., 2005), luni-solar and earth-tide gravitation model and 2 sinusoidal and 3 polynomial parameters (Hanuschak et al., 2005) to model periodic and slowly varying forces in the direction of the satellite roll axis (the latter is discussed below). Additional radiation pressure and atmospheric drag models were only used in the initialization phase when the drag-free control was not implemented.

In the science data collection phase, two types of non-gravitational perturbing accelerations were observed in the orbital motion. Both act along the roll axis of the GP-B satellite, since the roll of the satellite averages out any satellite body-fixed accelerations transverse to the roll axis. One perturbing acceleration is nearly constant each day, but gradually increasing over time. The other is nearly

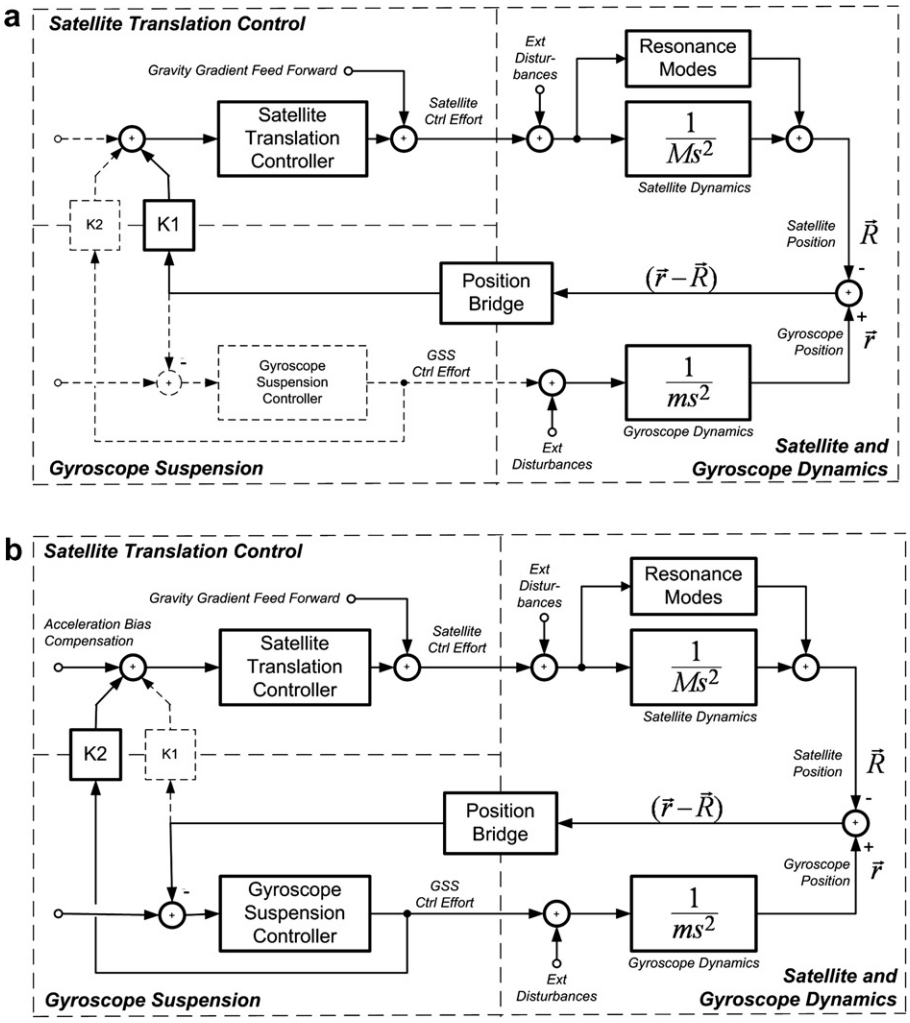

Fig. 3. Diagram of drag-free translation control system (a) free floating mode (b) accelerometer mode.

sinusoidal and oscillating at the frequency of the polhode motion of the gyroscope used as the proof mass. The polhode motion is a periodic motion of the gyroscope spin axis moving in the gyroscope body-fixed frame due to the difference of principal moments of inertia (Goldstein, 1980). As a result, the effects of sinusoidal and polynomial terms in the direction of the satellite roll axis must be included in the force modeling for an accurate orbit representation.

There is evidence indicating that some of the observed perturbing acceleration of the gyroscope used as the proof mass is due to interactions of electrical patch charges on the gyroscope and the housing. Those interior electrostatic forces as well as the exterior forces acting on the satellite tend to move the proof mass toward the housing and both must be compensated by thrusting to keep the proof mass centered in its housing. The non-gravitational force parameters in the orbit determination force model represent the axial component of the thrusting that compensates for just the interior forces. That thrusting, averaged over gyroscope spin period and satellite roll period, would be expected to have an axial resultant with both a constant component and a component with the polhode period that depends on the orientation of current gyroscope spin axis with respect to the satellite roll axis. The non-gravitational acceleration forces the satellite to follow a slightly non-gravitational trajectory.

Ground-based laser ranging measurements have been available since late July 2004. Because the laser ranging measurements are often sparse and ill-conditioned, it is frequently not possible to determine comparable orbits independently from the laser ranging measurements alone. Nevertheless, the laser ranging measurements are used to compute laser ranging residuals referenced to the orbit solutions determined from the GPS position data for an independent verification.

Additional information on force modeling for GP-B orbit determination and a description of the resulting GP-B orbit history were provided by Hanuschak et al. (2005) and Small (2006).

4. On-orbit performance

The non-gravitational perturbations varied during the flight, depending on whether the drag-free control was on

or off and which gyroscope was used as proof mass. Those effects on the orbit are most easily observed in the history of the semi-major axis, because small semi-major axis variations have corresponding effects on the orbit period which integrate into large in-track perturbations. Fig. 4 shows the history of the short-period mean semi-major axis of the GP-B orbit in the flight. In the initialization phase after the launch of the GP-B satellite on April 20, 2004 (day 111, all day numbers are measured from 00:00:00 UTC December 31, 2003), the drag-free control was off except for several tests. During that time it is seen that the semi-major axis decayed slowly mainly due to air drag. From the start of the science data collection on August 28, 2004 (day 241) to the depletion of the helium on September 29, 2005 (day 638), the drag-free control was implemented in the accelerometer mode as a baseline. During the drag-free portion of the mission the mean semi-major axis did not decay, but (because semi-major axis variations are proportional to perturbing acceleration components in the direction of the orbital velocity vector) it oscillated at a frequency which is the difference between the current polhode and orbital frequencies. It is seen in Fig. 4 that history was relatively stable except for two jumps. Around September 18, 2004 (day 262), the increasing polhode frequency of Gyroscope 3, then used as the proof mass, became equal to and then exceeded the orbital frequency. The corresponding oscillations of the mean semi-major axis then passed through a resonance, leading to an abrupt altitude decrease of about 140 m. The relatively large oscillations surrounding the resonance were greatly reduced on September 24, 2004 (day 268) when Gyroscope 1, which had a different polhode period, was designated as the proof mass. On March 4–8, 2005 (days 429–434) the drag-free control was turned off for 5 days after a reboot of the computer onboard the GP-B satellite, which resulted in a drag decay decrease of the semi-major axis by 9 m. The semi-major axis history and the higher-resolution details of the corresponding in-track perturbations proved useful in analyzing the history of the non-gravitational forces acting on the orbit (Small, 2006).

In the initialization phase, the drag-free translation control system was tested both in the free floating mode and in the accelerometer mode. Fig. 5 shows the control efforts of the proof mass, Gyroscope 3, and the control efforts of the satellite in the directions (which are fixed in the satellite body-fixed frame) along the satellite roll axis (Fig. 5a) and transverse to the satellite roll axis (Fig. 5b) in an example of drag-free control transition sequence on July 5, 2004 (day 187). As shown in the figure, the drag-free control system was initially off, and the control efforts of the satellite were zero. The control efforts of the gyroscope counteracted the gravity gradient on the gyroscope, which is a sinusoidal signal of twice orbital frequency in the direction along the roll axis and a sinusoidal signal of twice orbital frequency modulated at the roll frequency in the direction transverse to the roll axis. Then the drag-free control system was turned on in the accelerometer mode. The gyroscope suspension control was enabled, and the gyroscope control efforts were fed back into the drag-free control system. Note that the control efforts of the gyroscope used as the proof mass were near zero and the control efforts of the satellite counteracted the gravity gradient on the satellite. The drag-free control system was then switched to the free floating mode. The gyroscope suspension control was

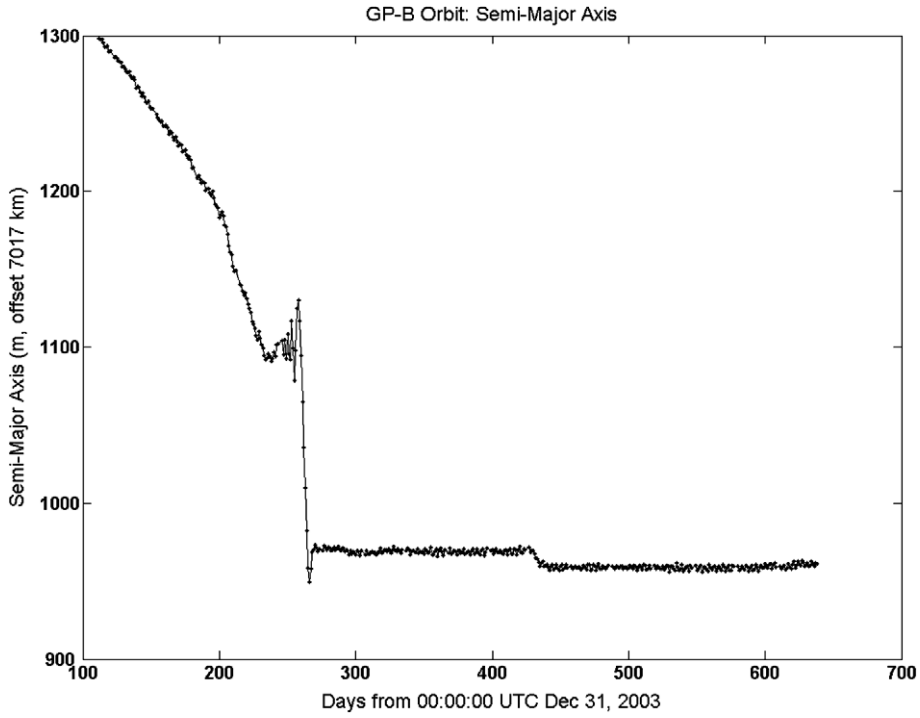

Fig. 4. History of semi-major axis of GP-B orbit in flight.

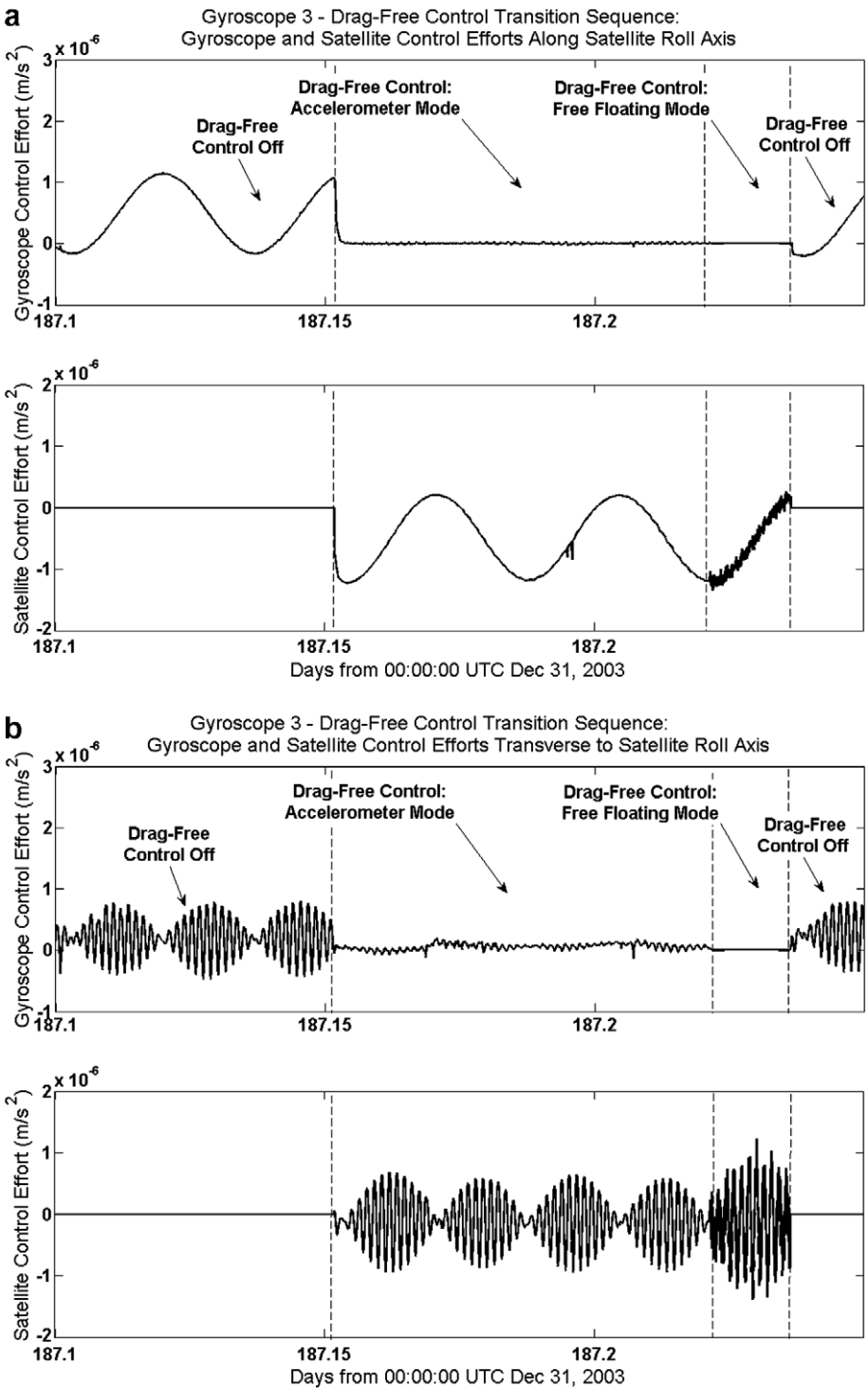

Fig. 5. An example of drag-free control transition sequence: gyroscope and satellite control efforts in the directions along (a) and transverse to (b) satellite roll axis (both directions are fixed in the satellite body-fixed frame).

disabled, and the control efforts of the proof mass were exactly zero. The drag-free control system flew the satellite around the position of the proof mass. Finally, the drag-free control system was turned off, and the counteraction of the gravity gradient can be seen again in the control efforts of the gyroscope.

Fig. 6 shows the spectra of the satellite control efforts and the gyroscope control efforts in the directions (which are in the orbital plane and fixed in inertial space) along the satellite roll axis (Fig. 6a and b) and transverse to the satellite roll axis (Fig. 6c and d). The data were from 14 days starting from July 19, 2005 (day 566), when the drag-free control was implemented in the accelerometer mode, and exhibit the representative performance of the drag-free translation control system of the GP-B satellite. In Fig. 6a and c, a peak at twice orbital

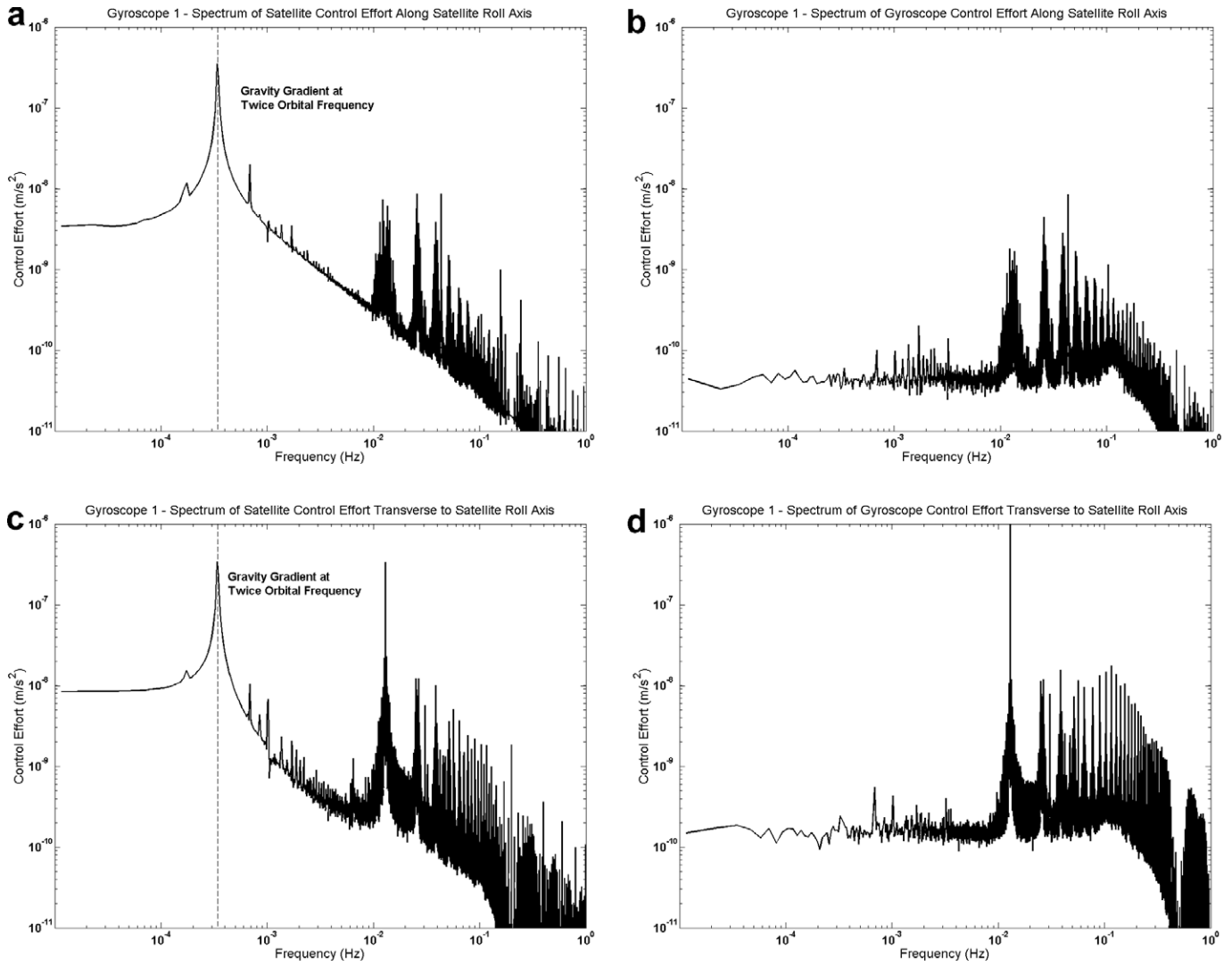

Fig. 6. Spectra of satellite control efforts and gyroscope control efforts in the directions along (a,b) and transverse to (c,d) satellite roll axis (both directions are in the orbital plane and fixed in inertial space. The data were from 14 days starting from July 19, 2005).

frequency can be seen in the spectrum of the satellite control effort due to the gravity gradient. Note that the residual accelerations from the gyroscope control efforts are less than 4×10^{-11} m/s^2 (along the satellite roll axis) and less than 2×10^{-10} m/s^2 (transverse to the satellite roll axis) between 0.01 mHz and 10 mHz in inertial space (averaging period: 24 h). It is observed that the drag-free control reduces the gravity gradient and environmental forces on the satellite to the noise level of the gyroscope control effort by a factor of about 10,000 along the satellite roll axis.

The estimated parameters in the orbit determination force model show that the amplitude of sinusoidal component of the perturbing acceleration varied from about 5×10^{-7} m/s^2 at the start of the science data collection phase to less than 1×10^{-8} m/s^2 near the end of the science data collection phase. Since the bias of the perturbing acceleration estimated in the orbit determination was uploaded to the satellite and added to the error signal commanding the drag-free control, the constant component of perturbing acceleration was kept below 1×10^{-7} m/s^2 in the science data collection phase. The non-gravitational perturbing acceleration of the GP-B satellite along the satellite roll axis causes the gyroscope spin axis to drift less than 9×10^{-5} arcsec/yr.

Fig. 7 shows RMS position vector differences (Fig. 7a) and RMS velocity vector differences (Fig. 7b) of the GP-B orbit solutions in the central 3-hour portions of the overlaps between subsequent data spans in the science data collection phase, demonstrating the quality of the GP-B orbit determination. The dominant position error is in-track and dominant velocity error is radial. (The position and velocity error plots are closely correlated because a small angular in-track error of $\delta\theta$ causes a radial velocity error of $V\delta\theta$ due to the rotation of the velocity vector V.) The error spikes near day 275 occurred because then the increasingly high-frequency in-track oscillations of the non-gravitational accelerations temporarily exceeded

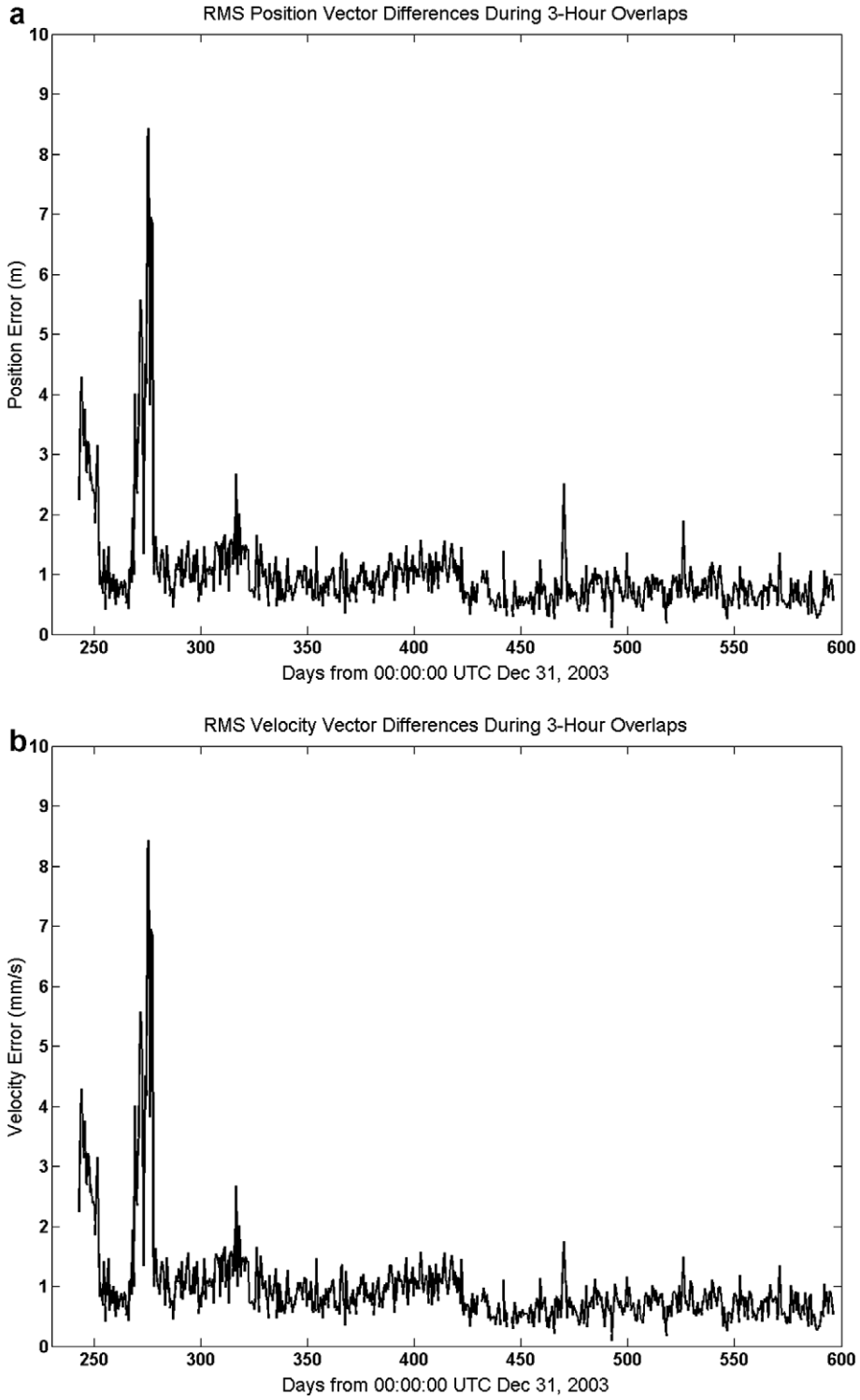

Fig. 7. RMS position vector differences (a) and RMS velocity vector differences (b) of GP-B orbit solutions in central 3-hour portions of overlaps between subsequent data spans in science data collection phase.

the resolution of the modeling parameters. It is observed that the ground processing of GPS position data provides orbit overlap solutions with position errors of 1.1 m (RMS) and velocity errors of 0.9 mm/s (RMS).

As an independent verification, Fig. 8 shows the laser ranging residuals referenced to the GP-B orbit solutions obtained from the GPS position data. It is observed that those residuals are at the level of 2.2 m (RMS). Those laser ranging measurements were not filtered except to discard outliers with residuals greater than 30 m, and they were not corrected for the 1.75 m offset between the laser reflector and the mass center of the GP-B satellite.

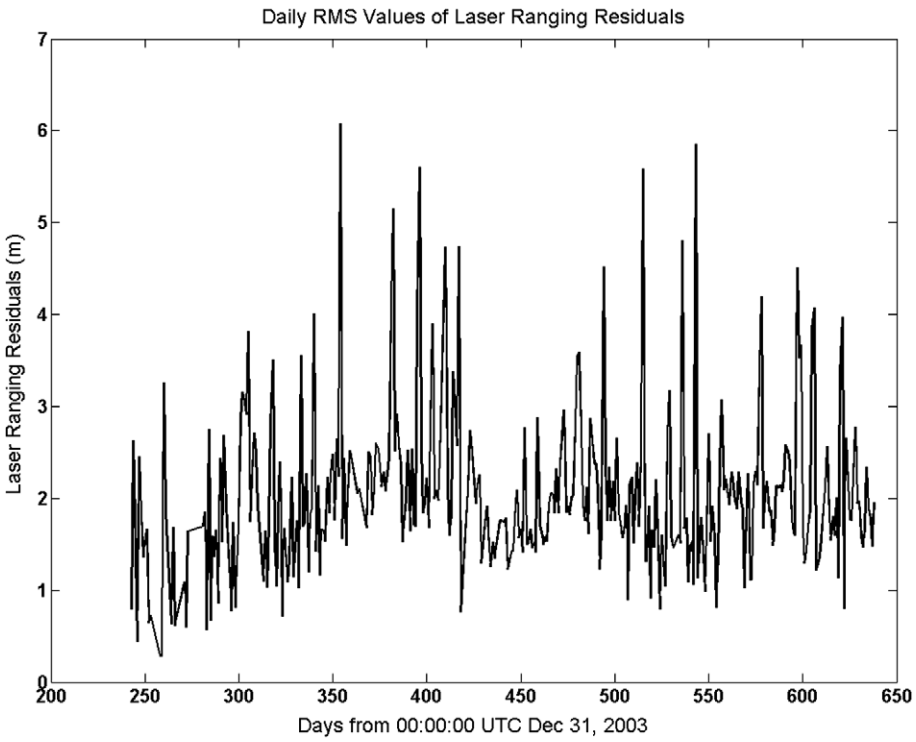

Fig. 8. Laser ranging residuals referenced to GPS-based orbit solutions.

5. Conclusions

The drag-free translation control system of the GP-B satellite was successfully demonstrated in the flight, both in the free floating mode and in the accelerometer mode. Its on-orbit performance satisfies the requirements of the GP-B science experiment. The residual accelerations from the gyroscope control efforts are less than 4×10^{-11} m/s^2 (along the satellite roll axis) and less than 2×10^{-10} m/s^2 (transverse to the satellite roll axis) between 0.01 mHz and 10 mHz in inertial space. The non-gravitational acceleration along the satellite roll axis, including a nearly constant component (which is kept below 1×10^{-7} m/s^2) and a sinusoidal component (whose amplitude varies from about 5×10^{-7} m/s^2 to less than 1×10^{-8} m/s^2), causes the gyroscope spin axis to drift less than 9×10^{-5} arcsec/yr. The GPS receivers onboard the GP-B satellite functioned well during the on-orbit experiment, providing real-time position, velocity and timing data. Overlap errors and laser ranging residuals indicate that ground processing of the GPS position data provides GP-B orbit solutions having RMS position and velocity errors of a few meters and a few mm/s, well within the RMS mission requirements of 25 m and 7.5 cm/s.

Acknowledgements

The GP-B experiment was accomplished under NASA funding, Contract No. NAS8-39225. The authors thank M. Adams and A. Ndili of Stanford University, K. Galal of NASA Ames Research Center, L. Herman of the Aerospace Corporation and J. Kirschenbaum of Lockheed Martin Company for their contributions to the development and flight of the GP-B drag-free translation control and orbit determination system.

References

Applied Physics Lab of John Hopkins University and Guidance and Control Lab of Stanford University. A satellite free of all but gravitational forces: TRIAD I. J. Spacecraft, 11(9), 637–644, 1974.

Bencze, W.J., DeBra, D.B., Herman, L., et al. On-orbit performance of the Gravity Probe B drag-free translation control system. Proc. 29th Guidance and Control Conference. American Astronautical Society, Breckenridge, Colorado, 2006.

DeBra, D.B. Drag-free control for fundamental physics missions. Adv. Space Res. 32 (7), 1221–1226, 2003.

Everitt, C.W.F. The Stanford relativity gyroscope experiment: history and overview, in: Fairbank, J.D., Deaver, B.S. Jr., Everitt, C.W.F., Michelson, P.F. (Eds.), Near Zero: New Frontiers of Physics. W.H Freeman & Co, New York, pp. 587–639, 1988.

Everitt, C.W.F., Buchman, S., DeBra, D.B., et al. Gravity Probe B: countdown to launch, in: Gyros, Clocks, Interferometers...: Testing Relativistic Gravity in Space. Springer, Berlin, pp. 52–82, 2001.

Goldstein, H. Classical Mechanics, second ed. Addison Wesley, New York, 207, 1980.

Hanuschak, G., Small, H., DeBra, D.B., et al. Gravity Probe B GPS orbit determination with verification by Satellite Laser Ranging. Proc. GNSS 2005 Meeting, The Institute of Navigation, Long Beach, CA, 2005.

Lange, B.O. The drag-free satellite. AIAA J 2 (9), 1590–1606, 1964.

Pearlman, M.R., Degnan, J.J., Bosworth, J.M. The International Laser Ranging Service. Adv. Space Res. 30 (2), 135–143, 2002.

Pugh, G.E. Proposal for a satellite test of the Coriolis prediction of general relativity. WSEG Research Memeorandum Number 11, Weapons Systems Evaluation Group, The Pentagon, Washington

D.C., November 12, 1959. Reprinted in: Ruffini, R.J., Sigismondi, C. (Eds.) Nonlinear Gravitodynamics: The Lense-Thirring Effect. World Scientific, New Jersey, 414–426, 2003.

Shestople, P., Li, J., Ndili, A., et al. Gravity Probe B GPS receivers. Proc. GNSS 2004 Meeting, The Institute of Navigation, Long Beach, CA, 2004.

Small, H. Axial thrusting effects on the GP-B orbit. GP-B Internal Report S1018, Gravity Probe B Project, Stanford University, Stanford, California, 2006.

Tapley, B., Ries, J., Bettadpur, S., et al. GGM02 – an improved Earth gravity field model from GRACE. J. Geodesy 79 (8), 467–478, 2005.